

Role of the Solar Minimum in the Waiting Time Distribution Throughout the Heliosphere

Yosia I Nurhan¹, Jay Robert Johnson¹, Jonathan R Homan¹, and Simon Wing²

¹Andrews University

²Johns Hopkins University

November 26, 2022

Abstract

Many processes throughout the heliosphere such as flares, CMEs, storms and substorms have abrupt onsets. The waiting time between these onsets provides key insights as to the underlying dynamical processes. We explore the tail of these waiting time distributions in the context of random processes driven by the solar magnetic activity cycle, which we approximate by a sinusoidal driver. Analytically, we find that the distribution of large waiting times of such a process approaches a power law slope of -2.5 at large enough waiting time, and we find that this power law is primarily controlled by the conditions when the driving is minimum. We find that the asymptotic behavior of the waiting time distributions of solar flares, coronal mass ejections, geomagnetic storms, and substorms exhibit power laws are in reasonable agreement with a sinusoidally driven nonstationary Poisson process.

12 **Abstract**

13 Many processes throughout the heliosphere such as flares, CMEs, storms and substorms
 14 have abrupt onsets. The waiting time between these onsets provides key insights as to
 15 the underlying dynamical processes. We explore the tail of these waiting time distribu-
 16 tions in the context of random processes driven by the solar magnetic activity cycle, which
 17 we approximate by a sinusoidal driver. Analytically, we find that the distribution of large
 18 waiting times of such a process approaches a power law slope of -2.5 at large enough wait-
 19 ing time, and we find that this power law is primarily controlled by the conditions when
 20 the driving is minimum. We find that the asymptotic behavior of waiting time distri-
 21 butions of solar flares, coronal mass ejections, geomagnetic storms, and substorms ex-
 22 hibit power laws are in reasonable agreement with a sinusoidally driven nonstationary
 23 Poisson process.

24 **Plain Language Summary**

25 Many events in the solar system are driven by the magnetic activity cycle of the
 26 sun. In this paper we show that for cyclical driving of a Poisson process that the prob-
 27 ability of the time between events satisfies a power law of -2.5 when the time between
 28 events is large. We show that this power law reasonably describes the distribution of wait-
 29 ing times for flares, CMEs, storms, and substorms at long waiting time. Additionally,
 30 we show that the distribution of long waiting times is primarily determined by the min-
 31 imum of the driving process.

32 **1 Introduction**

33 The solar cycle follows an 11-year cycle, characterized by fluctuations in the num-
 34 bers and surface area of sunspots, and impacts processes at the sun and throughout the
 35 heliosphere (Hathaway, 2010). Many processes that occur during the solar cycle can be
 36 identified as “events” because they are either localized in time or have a well defined on-
 37 set. Solar flares, coronal mass ejections (CMEs), geomagnetic storms, and geomagnetic
 38 substorms are among this class of processes.

39 It is well known that the dynamics of systems can be well described and reconstructed
 40 by considering the distribution of the set of time intervals of the system, $(\Delta_1, \Delta_2, \Delta, \dots, \Delta_N)$
 41 known as waiting times (Snelling et al., 2020; Aschwanden & McTiernan, 2010; Wheat-

land, 2000; Wheatland & Litvinenko, 2002; Wheatland, 2003; Consolini & Michelis, 2002). The waiting time distributions (WTDs) that are observed throughout the heliosphere may be governed by a combination of internal system dynamics and external driving by the magnetic activity cycle of the sun. If the events occur randomly, the process can be described as a Poisson process characterized by its rate. However, because many events throughout the heliosphere respond directly to the magnetic activity cycle, the activity cycle may modulate the rate of the events. As long as the response is random in nature, such processes can be described in terms of a nonstationary or time dependent Poisson process.

In general, the waiting time for solar flares, CMEs, storms, and substorms can be described by a nonstationary Poisson distribution, especially at large waiting times. Using Tsallis statistical mechanics, Balasis, Daglis, Anastasiadis, et al. (2011) suggested that the driving physical mechanisms of solar flares and storms have the same characteristics. Recently, Snelling et al. (2020) used information theory to show that while there is a short-term memory in the solar flare sequence, the distribution cannot be distinguished from a nonstationary Poisson distribution for longer waiting times. The WTD of CMEs have also been understood to follow a nonstationary Poisson process (Wheatland, 2003). CMEs, along with corotating interaction regions (CIRs), are the main drivers of storms. The CME-driven storms have a random occurrence pattern consistent with a nonstationary Poisson distribution. In contrast, CIR-driven storms have a periodicity of ~ 27 days. CIR-driven storms usually have a weaker intensity than CME-driven storms and happen during the declining phase of solar maximum (Tsubouchi & Omura, 2007; Borovsky & Denton, 2006). On average, the WTD of storms follows a nonstationary Poisson process (Tsubouchi & Omura, 2007). The WTD of substorms have two components: a non-random component which may correspond to spontaneous substorms with characteristic waiting time of ~ 2.5 hours and a random component which is fit by a Poisson distribution and generally occurs at waiting times longer than 5 hours (Borovsky et al., 1993).

The WTDs of these processes exhibit a power law for longer waiting times (heavy tail). For the WTD of solar flares at long waiting times, Boffetta et al. (1999) found a power law slope of -2.4 ± 0.1 . Wheatland (2000), restricting for flares of class C1 and above, found a power law slope of -2.16 ± 0.05 . Aschwanden and McTiernan (2010) found a power law in the tail of the WTD of solar flares with slope of ~ -2 . Wheatland (2003) found that the distribution of waiting times of CMEs in the Large Angle and Spectrometric Coronagraph (LASCO) CME catalog for the years 1996-2001 exhibit a power law

75 tail of -2.36 ± 0.11 for ($\Delta t > 10$ hours). Using Dst index from World Data Center
 76 for Geomagnetism, Kyoto University, Japan, Tsubouchi and Omura (2007) fitted the tail
 77 of the WTD for geomagnetic storms ($Dst < -100$ nT and $\Delta > 48$ hours) for $\Delta t >$
 78 1000 hours with a power law of -2.2 ± 0.1 .

79 Some have proposed different driver mechanisms of the nonstationary Poisson dis-
 80 tribution of the WTD of solar flares and explored their consequence to the behavior of
 81 the power law slope. Wheatland (2003) proposed that the flaring rate of solar flares fol-
 82 lows an exponential distribution and showed analytically that the WTDs of such non-
 83 stationary Poisson processes follow a power law of -3. Aschwanden and McTiernan (2010)
 84 further studied several different drivers and the power law resulted shown in Figure 2.

85 Wheatland and Litvinenko (2002) showed that the power law slope of WTDs varies
 86 with the solar cycle. Since the solar cycle is approximately sinusoidal, we propose that
 87 the flaring rate of solar flares follows the sinusoidal distribution to the first order. Here,
 88 we will show analytically how the observed power law behavior originates from the si-
 89 nusoidal rate and specifically the minima.

90 2 Waiting time statistics

From Aschwanden and McTiernan (2010), the waiting time probability distribu-
 tion for a nonstationary Poisson process with continuous flaring rate $\lambda(t)$ is approximately
 given by the equation

$$P(\Delta) = \frac{\int_0^T \lambda(t)^2 e^{-\lambda(t)\Delta} dt}{\int_0^T \lambda(t) dt}. \quad (1)$$

Suppose we choose a sinusoidal dependence of the flaring rate

$$\lambda(t) = \lambda_0(1 + \cos \omega t) \quad (2)$$

for which

$$\lambda_0 = \frac{1}{T} \int_0^T \lambda(t) dt. \quad (3)$$

is the average rate. Because this is a periodic signal, the statistics can all be obtained
 considering the process only over the interval $[0, T]$ where $T = 2\pi/\omega$. Then

$$P(\Delta) = \frac{\lambda_0 e^{-\lambda_0 \Delta}}{T} \int_0^T (1 + \cos(\omega t))^2 e^{-\lambda_0 \cos(\omega t) \Delta} dt. \quad (4)$$

Changing variables of integration $\theta = \omega t$ with $d\theta = \omega dt$, we have

$$P(\Delta) = \frac{\lambda_0 e^{-\lambda_0 \Delta}}{\omega T} \int_0^{2\pi} (1 + \cos(\theta))^2 e^{-\lambda_0 \cos(\theta) \Delta} d\theta. \quad (5)$$

The integral can be performed using the Bessel function identity (Abramowitz and Stegun (1972) - 9.6.34)

$$e^{z \cos \theta} = \sum_{n=-\infty}^{\infty} I_n(z) e^{in\theta} \quad (6)$$

so that

$$e^{-\lambda_0 \Delta \cos \theta} = \sum_{n=-\infty}^{\infty} I_n(-\lambda_0 \Delta) e^{in\theta} = \sum_{n=-\infty}^{\infty} (-1)^n I_n(\lambda_0 \Delta) e^{in\theta} \quad (7)$$

where

$$I_n(-z) = (-1)^n I_n(z) \text{ (Abramowitz and Stegun (1972) - 9.6.30)}. \quad (8)$$

Then

$$P(\Delta) = \lambda_0 e^{-\lambda_0 \Delta} \sum_{n=-\infty}^{\infty} (-1)^n I_n(\lambda_0 \Delta) \frac{1}{2\pi} \int_0^{2\pi} e^{in\theta} \left(1 + \frac{e^{i\theta} + e^{-i\theta}}{2}\right)^2 d\theta \quad (9)$$

$$= \lambda_0 e^{-\lambda_0 \Delta} \sum_{n=-\infty}^{\infty} (-1)^n I_n(\lambda_0 \Delta) \left[\frac{1}{2\pi} \int_0^{2\pi} e^{in\theta} \left(1 + e^{i\theta} + e^{-i\theta} + \frac{e^{2i\theta} + 2 + e^{-2i\theta}}{4}\right) d\theta \right] \quad (10)$$

$$= \lambda_0 e^{-\lambda_0 \Delta} \sum_{n=-\infty}^{\infty} (-1)^n I_n(\lambda_0 \Delta) \left[\frac{3}{2} \delta_{n,0} + \delta_{n,-1} + \delta_{n,1} + \frac{1}{4} (\delta_{n,-2} + \delta_{n,2}) \right] \quad (11)$$

$$= \lambda_0 e^{-\lambda_0 \Delta} \left[\frac{3}{2} I_0(\lambda_0 \Delta) - I_{-1}(\lambda_0 \Delta) - I_1(\lambda_0 \Delta) + \frac{1}{4} (I_{-2}(\lambda_0 \Delta) + I_2(\lambda_0 \Delta)) \right] \quad (12)$$

and making use of the property

$$I_{-n}(z) = I_n(z), \text{ (Abramowitz and Stegun (1972) - 9.6.6)}, \quad (13)$$

we find the analytic solution

$$P(\Delta) = \lambda_0 e^{-\lambda_0 \Delta} \left[\frac{3}{2} I_0(\lambda_0 \Delta) - 2I_1(\lambda_0 \Delta) + \frac{1}{2} I_2(\lambda_0 \Delta) \right]. \quad (14)$$

Now we perform the asymptotic analysis. For large Δ we have

$$I_n(z) \sim \frac{e^z}{\sqrt{2\pi z}} \left[1 - \frac{\mu-1}{8z} + \frac{(\mu-1)(\mu-9)}{2!(8z)^2} - \frac{(\mu-1)(\mu-9)(\mu-25)}{3!(8z)^3} + \dots \right] \quad (15)$$

where $\mu = 4n^2$. And so

$$I_0(z) e^{-z} \sim \frac{1}{\sqrt{2\pi z}} \left[1 + \frac{1}{8z} + \frac{9}{128z^2} + \dots \right] \quad (16)$$

$$I_1(z) e^{-z} \sim \frac{1}{\sqrt{2\pi z}} \left[1 - \frac{3}{8z} - \frac{15}{128z^2} + \dots \right] \quad (17)$$

$$I_2(z) e^{-z} \sim \frac{1}{\sqrt{2\pi z}} \left[1 - \frac{15}{8z} + \frac{105}{128z^2} + \dots \right]. \quad (18)$$

Therefore,

$$P(\Delta) \sim \lambda_0 \frac{1}{\sqrt{2\pi\lambda_0\Delta}} \left[\frac{3}{4(\lambda_0\Delta)^2} + \dots \right] \sim \lambda_0 \frac{3}{8} \sqrt{\frac{2}{\pi}} (\lambda_0\Delta)^{-2.5}. \quad (19)$$

91 So, in this case the power law is -2.5 . In the next section we will show how the power
 92 law can be derived from the minima of the rate function, a more general case.

93 We confirm our findings by numerically integrating Eq. (5). We then plot the nu-
 94 merical and analytic solutions in Figure 1. The third plot is the “local” power slope cal-
 95 culated by numerically differentiating $P(\Delta)/\lambda_0$. It can be seen that the power law slope
 96 approaches -2.5 asymptotically from below.

97 3 Role of the Minima

The WTD at large waiting times is mainly governed by the minima of the driver.
 As such, we will show how the minima affects the WTD at large waiting times. As be-
 fore, from Aschwanden and McTiernan (2010), for the nonstationary Poisson process with
 continuous $\lambda(t)$ we have approximately

$$P(\Delta) = \frac{\int_0^T \lambda(t)^2 e^{-\lambda(t)\Delta} dt}{\int_0^T \lambda(t) dt}.$$

Let λ be normalized to λ_0 :

$$\lambda = \lambda_0 \cdot g(t). \quad (20)$$

Then

$$P(\Delta) = \lambda_0 \int_0^T g(t)^2 e^{-\lambda_0 \Delta g(t)} dt. \quad (21)$$

Suppose $g(t)$ has a minimum at $t = t_0$:

$$g(t) \approx g(t_0) + \frac{g''(t_0)}{2!} (t - t_0)^2 + \dots \quad (22)$$

Then,

$$P(\Delta) = \lambda_0 \int_0^T [g(t_0) + \frac{g''(t_0)}{2!} (t - t_0)^2 + \dots]^2 e^{-\lambda_0 \Delta [g(t_0) + \frac{g''(t_0)}{2!} (t - t_0)^2 + \dots]} dt. \quad (23)$$

Let $\alpha = t - t_0$ and $g_0 = g(t_0)$. As long as t_0 is in the interval,

$$P(\Delta) \sim \lambda_0 \int_{-\infty}^{\infty} [g_0 + \frac{g_0''}{2} \alpha^2]^2 e^{-\lambda_0 \Delta [g_0 + \frac{g_0''}{2} \alpha^2]} d\alpha \quad (24)$$

$$\sim \lambda_0 e^{-\lambda_0 \Delta g(0)} \int_{-\infty}^{\infty} [g_0 + \frac{g_0''}{2} \alpha^2]^2 e^{-\frac{\lambda_0 \Delta g_0''}{2} \alpha^2} d\alpha. \quad (25)$$

Let $\mu_0 = \frac{\lambda_0 \Delta}{2}$,

$$P(\Delta) \sim \lambda_0 e^{-2\mu_0 g_0} \int_{-\infty}^{\infty} [g_0^2 + g_0 g_0'' \alpha^2 + \frac{g_0''^2}{4} \alpha^4] e^{-\mu_0 g_0'' \alpha^2} d\alpha \quad (26)$$

$$\sim \lambda_0 e^{-2\mu_0 g_0} [g_0^2 \sqrt{\frac{\pi}{g_0''}} \mu_0^{-1} + \frac{g_0}{2} \sqrt{\frac{\pi}{g_0''}} \mu_0^{-1.5} + \frac{3}{16} \sqrt{\frac{\pi}{g_0''}} \mu_0^{-2.5}] \quad (27)$$

$$\sim \lambda_0 e^{-2\mu_0 g_0} \sqrt{\frac{\pi}{g_0''}} [g_0^2 \mu_0^{-1} + \frac{g_0}{2} \mu_0^{-1.5} + \frac{3}{16} \mu_0^{-2.5}] \quad (28)$$

98 It can be seen that when the rate vanishes at the minimum ($g_0 = 0$), the power law will
 99 be -2.5 . When the rate at the minimum is small there will be a range where the $\mu^{-2.5}$
 100 term dominates. In this range, we expect ($\Delta \ll 1/\lambda_0$) and the WTD will have a -2.5
 101 power law; otherwise, other power laws may be more applicable. In some processes, the
 102 sinusoidal rate minima might be elevated (nonzero). We derive the analytic solution for
 103 an sinusoidal rate function with an elevated minima in the Appendix A.

104 4 Data Analysis

105 We present analyses of the waiting time distributions of four different processes:
 106 solar flares, CMEs, storms, and substorms. We calculate the waiting time probability
 107 distribution using logarithmic binning and plot them alongside the power law fit from
 108 equation (14) (see Figure 3).

109 4.1 Solar Flares

110 The solar flare data was obtained from the Geostationary Operational Environmen-
 111 tal Satellite (GOES) catalog of flares from 1975-2017, available from [https://www.ngdc](https://www.ngdc.noaa.gov/stp/solar/solarflares.html)
 112 [.noaa.gov/stp/solar/solarflares.html](https://www.ngdc.noaa.gov/stp/solar/solarflares.html). In keeping with previous studies by Snelling
 113 et al. (2020), we used flares with a minimum peak flux greater than 1.4×10^{-6} , namely
 114 flares of C1 class and above. Event times were set to be the time of the maximum flux.
 115 From this sequence consisting of 71,595 flares, we construct a sequence of waiting times.
 116 This solar flares waiting time series was the same series analyzed by Snelling et al. (2020).

117 4.2 CME

118 The Coronal Mass Ejection (CME) list was obtained from the Center for Solar Physics
 119 and Space Weather/Naval Research Laboratory (SOHO/LASCO) CME catalog [https://](https://cdaw.gsfc.nasa.gov/CME_list/)
 120 cdaw.gsfc.nasa.gov/CME_list/ from 1996 to 2020. We construct a sequence of wait-
 121 ing times from a sequence of 30,321 events.

122

4.3 Storms

123

124

125

126

127

128

129

130

131

The Dst record was obtained from the GSFC/SPDF OMNIWeb interface at <https://omniweb.gsfc.nasa.gov>. Using the hourly Dst index between 1963 and 2020, we define the onset of a storm event to be when the index goes below -50 nT and the end of a storm event to be when the index surpasses -20 nT. The choice of the minimum Dst index is to choose at least moderate storms events ($-100 \text{ nT} < Dst < -50 \text{ nT}$) as characterized in previous study by Balasis, Daglis, Papadimitriou, et al. (2011). Watari and Watanabe (1998) also chose $Dst < -50 \text{ nT}$ as a threshold for storms event. Event times were set to be the onset of the storm. From this sequence of 1276 storm events, we construct a sequence of waiting times.

132

4.4 Substorms

133

134

135

The substorms list was obtained from the SuperMAG substorms list at <http://supermag.jhuapl.edu/mag/>. We created our waiting time sequence from the substorms event times list between 1975 and 2019, which was composed of 68,878 events.

		α	$\Delta_{min}(\text{hours})$	$\Delta_{max}(\text{hours})$	χ^2	p
Solar Flares	Data	-2.74 ± 0.06	20	103	0.42	$\ll 0.001$
	Analytic Solution	-2.65 ± 0.05	20	103	0.038	$\ll 0.001$
CMEs	Data	-2.98 ± 0.05	20	189	1.03	$\ll 0.001$
	Analytic Solution	-2.68 ± 0.05	20	189	0.098	$\ll 0.001$
Storms	Data	-2.49 ± 0.15	566	4496	0.38	$\ll 0.001$
	Analytic Solution	-2.60 ± 0.2	566	4496	0.053	$\ll 0.001$
Substorms	Data	-2.40 ± 0.06	25	99	1.1	$\ll 0.001$
	Analytic Solution	-2.61 ± 0.13	25	99	0.0048	$\ll 0.001$

Table 1: Linear least squares fit for the WTDs of data and analytic solution, eq. 14, where the fitted power law is for $\Delta_{min} < \Delta < \Delta_{max}$.

5 Results and Discussions

Figure 3 plots waiting time distribution for solar flares, CMEs, storms, and substorms. The figure shows the existence of power laws for $\Delta_{min} < \Delta < \Delta_{max}$ region as described in Table 1. The power law distribution does not fit the actual WTD for the entire tail domain of the datasets perhaps due to some underlying dynamics that compete with the cyclical behavior. For the solar flares, it seems that the WTD at long waiting times may have a shallower slope. It may be the case that during solar minima, there are impulsive events which have been associated with shallower power law slope (Aschwanden & McTiernan, 2010). The power law slope of the CMEs is somewhat steeper than the WTD derived from the sinusoidal rate. Steeper slopes can be found when the minima of the sinusoidal rate is elevated (See Appendix A). If analyzed segment by segment, Wheatland (2003) found a power law $\alpha \sim -2.36 \pm 0.11$ for CMEs between 1996-2001, the period of lowest CMEs activity but found a power law $\alpha \sim -2.98 \pm 0.20$ for the years of 1999-2001, a period of higher activity where the minima of the rate function is elevated. These power laws are reasonably similar to the analytic distribution. However, there is a small difference, suggesting that additional processes should be considered beyond simple sinusoidal driving. For the substorms, the internal magnetospheric dynamics likely affects the distribution at shorter waiting times, thus the power law only matches at long waiting time. The sudden steepness of the slope for $\Delta > 100$ hrs may be attributed to the elevated minima of the rate function (see Appendix A). The power law distribution for the storms fits much better than for the substorms, indicating that the cyclical behavior of the external driver is generally more important. In other words, there is less internal dynamics involved than for substorms.

Although this paper focuses mostly on events impacted by the periodicity of the solar activity, the waiting time distribution of any nonstationary Poisson process that has a sinusoidal rate with a minimum near zero will have a power law of -2.5 at large waiting times. Even more generally, for any nonstationary Poisson processes that has a continuous rate with a minimum close to zero, the WTD will have a power law of -2.5 at large waiting times as long as the minimum rate is small, although natural processes might not reach that asymptotic point due to the rarity of the events at large waiting time and/or data gaps. Also, for processes with an elevated minima, the slope at large waiting times may steepen dramatically and drop off exponentially. It may be inferred that, for longer waiting times, the internal dynamics may be a lot less important than

169 what is driving the system. In this case, it is the characteristics of the driver at its min-
 170 imum.

171 The power laws of WTDs are often thought to result from SOC processes or tur-
 172 bulent interactions. While SOC models predict a Poisson distribution, variable driving
 173 of SOC models results in a nonstationary Poisson distribution characterized by a power
 174 law at long waiting times (Aschwanden, 2019). In this work we have shown that sim-
 175 ple periodic driving of a system with a random response can produce a power law of -
 176 2.5. Because the solar magnetic activity cycle is a primary driver of dynamics through-
 177 out the solar system, it is not surprising that such power laws are seen in solar flares,
 178 CME, storm and substorm datasets. It is also to be noted that because long waiting times
 179 primarily occur when the rate is minimum, that the tail of power laws provide informa-
 180 tion about conditions at the minima in activity cycles, and may provide insight as to the
 181 underlying dynamics at solar minima and the overlap between cycles (McIntosh et al.,
 182 2020).

183 **Acknowledgments**

184 The solar flare data was obtained from the Geostationary Operational Environmental
 185 Satellite (GOES) catalog of flares from 1975-2017, available from [https://www.ngdc.noaa](https://www.ngdc.noaa.gov/stp/solar/solarflares.html)
 186 [.gov/stp/solar/solarflares.html](https://www.ngdc.noaa.gov/stp/solar/solarflares.html). The Coronal Mass Ejection (CME) list was ob-
 187 tained from the Center for Solar Physics and Space Weather/Naval Research Labora-
 188 tory (SOHO/LASCO) CME catalog https://cdaw.gsfc.nasa.gov/CME_list/ from 1996
 189 to 2020. The *Dst* record was obtained from the GSFC/SPDF OMNIWeb interface at
 190 <https://omniweb.gsfc.nasa.gov>. The substorms list was obtained from the Super-
 191 MAG substorms list at <http://supermag.jhuapl.edu/mag/>. This work is supported
 192 by NASA grants NNX15AJ01G, NNX15AB17I, NNX16AQ87G, 80NSSC19K0270, 80NSSC19K0843,
 193 80NSSC18K0835, 80NSSC20K0355, NNX17AI50G, NNX17AI47G, 80HQTR18T0066,
 194 80NSSC20K0704 and NSF grants AGS1832207 and AGS1602855 and Andrews Univer-
 195 sity FRG 201119.

196 **References**

197 Abramowitz, M., & Stegun, I. A. (1972). *Handbook of mathematical functions with*
 198 *formulas, graphs, and mathematical tables*. National Bureau of Standards, Ap-
 199 plied Mathematics Series.

- 200 Aschwanden, M. J. (2019, dec). Nonstationary fast-driven, self-organized criticality
201 in solar flares. *The Astrophysical Journal*, *887*(1), 57. doi: 10.3847/1538-4357/
202 ab5371
- 203 Aschwanden, M. J., & McTiernan, J. M. (2010, jun). Reconciliation of waiting
204 time statistice of solar flares observed in hard x-rays. *The Astrophysical Jour-*
205 *nal*, *717*(2), 683–692. doi: 10.1088/0004-637x/717/2/683
- 206 Balasis, G., Daglis, I. A., Anastasiadis, A., Papadimitriou, C., Manda, M., & Eftax-
207 ias, K. (2011, jan). Universality in solar flare, magnetic storm and earthquake
208 dynamics using tsallis statistical mechanics. *Physica A: Statistical Mechanics*
209 *and its Applications*, *390*(2), 341–346. doi: 10.1016/j.physa.2010.09.029
- 210 Balasis, G., Daglis, I. A., Papadimitriou, C., Anastasiadis, A., Sandberg, I., & Eftax-
211 ias, K. (2011, oct). Quantifying dynamical complexity of magnetic storms and
212 solar flares via nonextensive tsallis entropy. *Entropy*, *13*(10), 1865–1881. doi:
213 10.3390/e13101865
- 214 Boffetta, G., Carbone, V., Giuliani, P., Veltri, P., & Vulpiani, A. (1999, nov). Power
215 laws in solar flares: Self-organized criticality or turbulence? *Physical Review*
216 *Letters*, *83*(22), 4662–4665. doi: 10.1103/physrevlett.83.4662
- 217 Borovsky, J. E., & Denton, M. H. (2006). Differences between CME-driven storms
218 and CIR-driven storms. *Journal of Geophysical Research*, *111*(A7). doi: 10
219 .1029/2005ja011447
- 220 Borovsky, J. E., Nemzek, R. J., & Belian, R. D. (1993, mar). The occurrence
221 rate of magnetospheric-substorm onsets: Random and periodic substorms.
222 *Journal of Geophysical Research: Space Physics*, *98*(A3), 3807–3813. doi:
223 10.1029/92ja02556
- 224 Consolini, G., & Michelis, P. D. (2002, dec). Fractal time statistics of AE-index
225 burst waiting times: evidence of metastability. *Nonlinear Processes in Geo-*
226 *physics*, *9*(5/6), 419–423. doi: 10.5194/npg-9-419-2002
- 227 Hathaway, D. H. (2010, mar). The solar cycle. *Living Reviews in Solar Physics*,
228 *7*(1). doi: 10.12942/lrsp-2010-1
- 229 McIntosh, S. W., Chapman, S., Leamon, R. J., Egeland, R., & Watkins, N. W.
230 (2020, nov). Overlapping magnetic activity cycles and the sunspot num-
231 ber: Forecasting sunspot cycle 25 amplitude. *Solar Physics*, *295*(12). doi:
232 10.1007/s11207-020-01723-y

- 233 Snelling, J. M., Johnson, J. R., Willard, J., Nurhan, Y., Homan, J., & Wing, S.
 234 (2020, aug). Information theoretical approach to understanding flare wait-
 235 ing times. *The Astrophysical Journal*, *899*(2), 148. doi: 10.3847/1538-4357/
 236 aba7b9
- 237 Tsubouchi, K., & Omura, Y. (2007). Long-term occurrence probabilities of in-
 238 tense geomagnetic storm events. *Space Weather*, *5*, n/a-n/a. doi: 10.1029/
 239 2007sw000329
- 240 Watari, S., & Watanabe, T. (1998, jul). The solar drivers of geomagnetic distur-
 241 bances during solar minimum. *Geophysical Research Letters*, *25*(14), 2489–
 242 2492. doi: 10.1029/98gl01085
- 243 Wheatland, M. S. (2000, jun). The origin of the solar flare waiting-time distribution.
 244 *The Astrophysical Journal*, *536*(2), L109–L112. doi: 10.1086/312739
- 245 Wheatland, M. S. (2003). The coronal mass ejection waiting-time distribution. *Solar*
 246 *Physics*, *214*(2), 361–373. doi: 10.1023/a:1024222511574
- 247 Wheatland, M. S., & Litvinenko, Y. E. (2002). Understanding solar flare
 248 waiting-time distributions. *Solar Physics*, *211*(1/2), 255–274. doi:
 249 10.1023/a:1022430308641

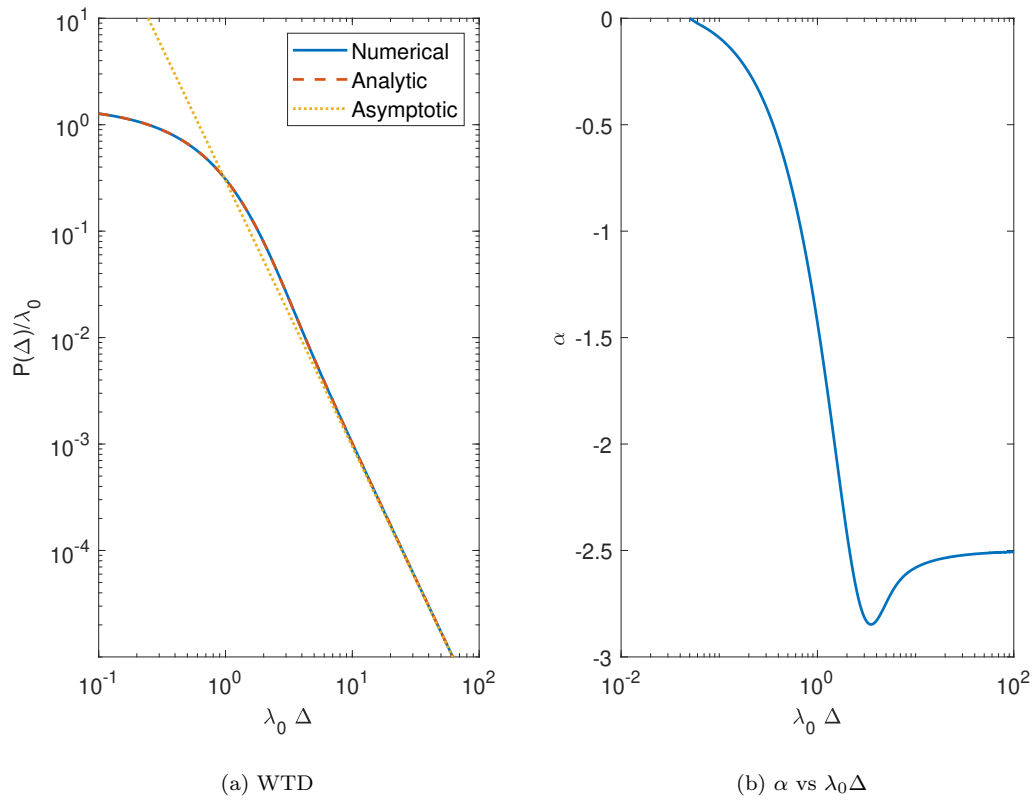


Figure 1: (a) is a plot of numerical and analytic solutions to eq. (5). The asymptotic solution is $P(\Delta)/\lambda_0 \sim (\lambda_0 \Delta)^{-2.5}$. Plot (b) is the “local” power law estimation.

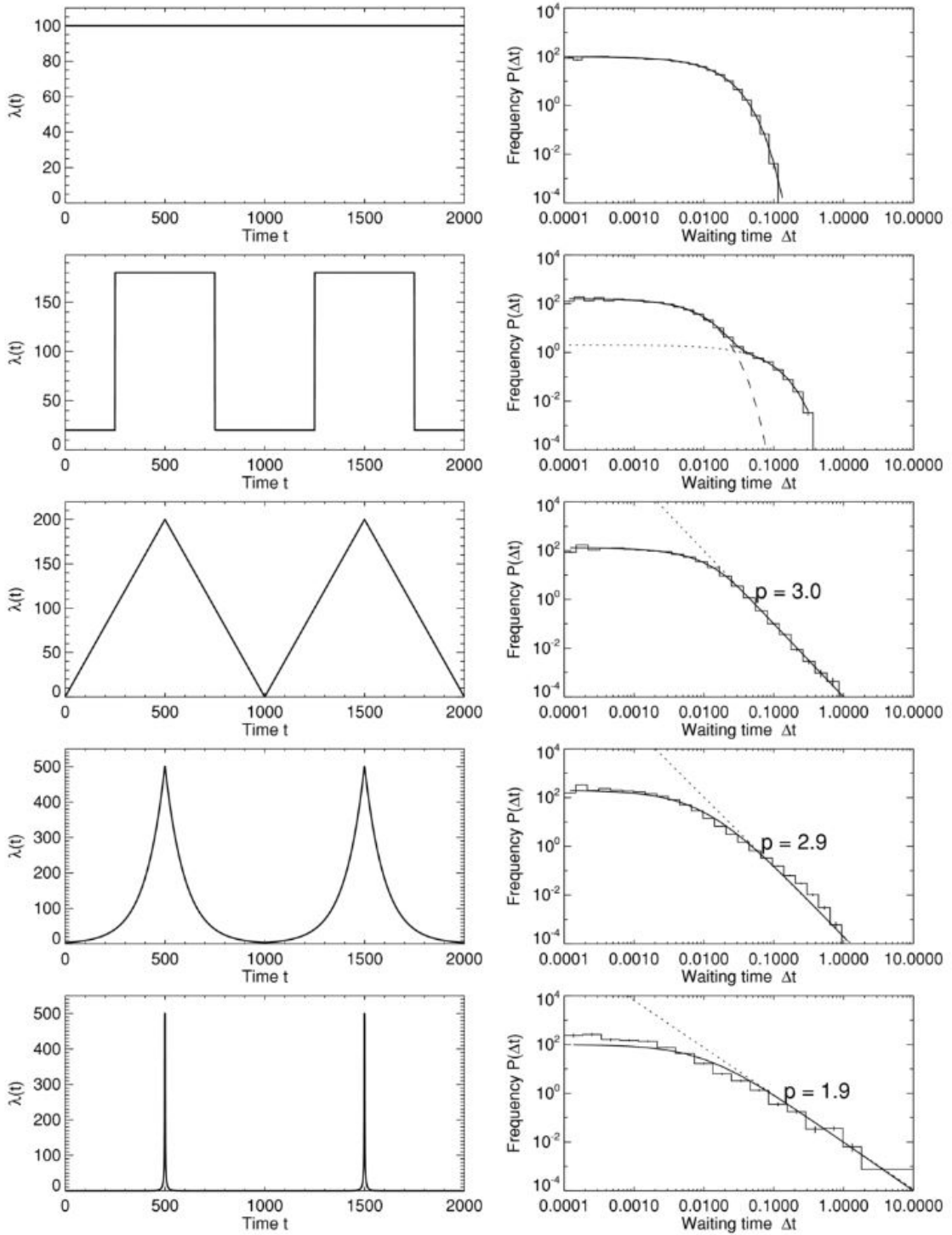


Figure 2: Figure from Aschwanden and McTiernan (2010). The rate functions, $\lambda(t)$, are shown on the left side, and the corresponding waiting time distributions are shown on the right hand side. Power law fits are indicated with a dotted line where p is the power law slope.

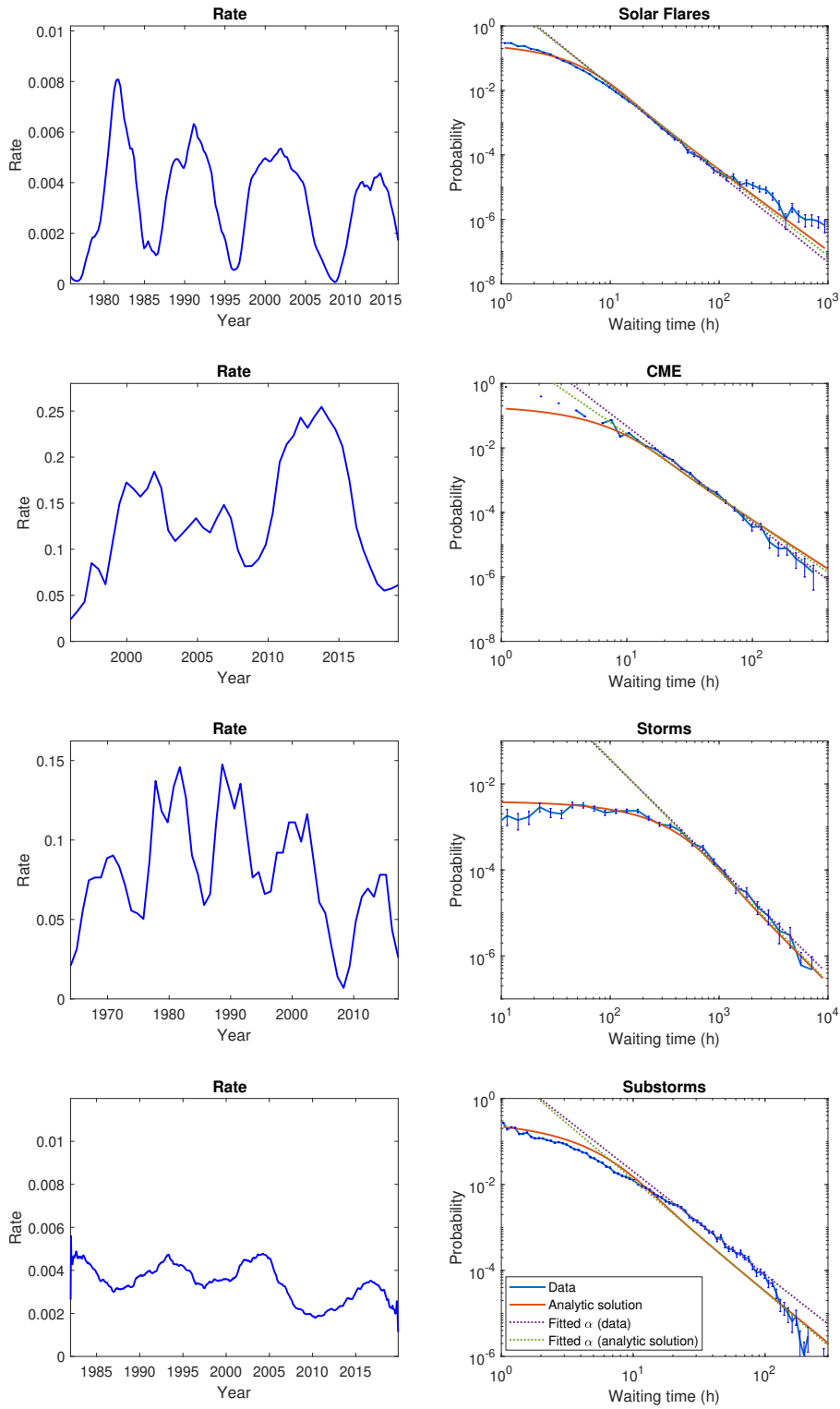


Figure 3: Waiting time probability distribution and rate over the years of the solar, CMEs, Storms and Substorm data. The power law estimate α is over a range as described in table 1

251 **Appendix A Sinusoidal Rate Function with Elevated Minimum, $\lambda_{min} >$**
 252 **0**

253 For the nonstationary Poisson process we have approximately:

$$P(\Delta) = \frac{\int_0^T \lambda(t)^2 e^{-\lambda(t)\Delta} dt}{\int_0^T \lambda(t) dt}. \quad (\text{A1})$$

Suppose we choose a sinusoidal dependence and consider a period (it will be the same result for multiple periods):

$$\lambda(t) = \lambda_0 \left(1 + \frac{\beta}{2} \cos \omega t \right) \quad (\text{A2})$$

where

$$\delta\lambda = \lambda_{max} - \lambda_{min} = \beta\lambda_0 \quad (\text{A3})$$

For which

$$\int_0^T \lambda(t) dt = \lambda_0 T \quad (\text{A4})$$

when integrated over a period. Then we have

$$P(\Delta) = \frac{\lambda_0 e^{-\lambda_0 \Delta}}{T} \int_0^T \left(1 + \frac{\beta}{2} \cos \omega t \right)^2 e^{-\frac{\beta\lambda_0 \Delta}{2} \cos(\omega t)} dt. \quad (\text{A5})$$

Changing variables of integration:

$$\theta = \omega t$$

with

$$d\theta = \omega dt$$

$$P(\Delta) = \frac{\lambda_0 e^{-\lambda_0 \Delta}}{\omega T} \int_0^{\omega T} \left(1 + \frac{\beta}{2} \cos(\theta) \right)^2 e^{-b \cos(\theta) \Delta} d\theta$$

where $b = \frac{\lambda_0 \beta \Delta}{2}$. Because this is a periodic signal, the statistics can all be obtained by considering one period. Let us consider $P(\Delta)$ determined over a period $\omega T = 2\pi$. Then

$$P(\Delta) = \frac{\lambda_0 e^{-\lambda_0 \Delta}}{2\pi} \int_0^{2\pi} \left(1 + \frac{\beta}{2} \cos \theta \right)^2 e^{-b \cos \theta} d\theta. \quad (\text{A6})$$

The integral can be performed using the Bessel function identity ((Abramowitz & Stegun, 1972) - 9.6.34)

$$e^{z \cos \theta} = \sum_{n=-\infty}^{\infty} I_n(z) e^{in\theta} \quad (\text{A7})$$

so that

$$e^{-b \cos \theta} = \sum_{n=-\infty}^{\infty} I_n(-b)e^{in\theta} = \sum_{n=-\infty}^{\infty} (-1)^n I_n(b)e^{in\theta} \quad (\text{A8})$$

where

$$I_n(-z) = (-1)^n I_n(z) \quad (\text{Abramowitz \& Stegun, 1972} - 9.6.30). \quad (\text{A9})$$

Then

$$P(\Delta) = \lambda_0 e^{-\lambda_0 \Delta} \sum_{n=-\infty}^{\infty} I_n(b) \frac{1}{2\pi} \int_0^{2\pi} e^{in\theta} \left(1 + \frac{\beta}{2} \left(\frac{e^{i\theta} + e^{-i\theta}}{2} \right) \right)^2 d\theta \quad (\text{A10})$$

$$= \lambda_0 e^{-\lambda_0 \Delta} \sum_{n=-\infty}^{\infty} (-1)^n I_n(b) \left[\frac{1}{2\pi} \int_0^{2\pi} e^{in\theta} \left(1 + \frac{\beta}{2} (e^{i\theta} + e^{-i\theta}) + \frac{\beta^2}{4} \left(\frac{e^{2i\theta} + 2 + e^{-2i\theta}}{4} \right) \right) d\theta \right] \quad (\text{A11})$$

$$= \lambda_0 e^{-\lambda_0 \Delta} \sum_{n=-\infty}^{\infty} (-1)^n I_n(b) \left[\left(1 + \frac{\beta^2}{8} \right) \delta_{n,0} + \frac{\beta}{2} (\delta_{n,-1} + \delta_{n,1}) + \frac{\beta^2}{16} (\delta_{n,-2} + \delta_{n,2}) \right] \quad (\text{A12})$$

$$= \lambda_0 e^{-\lambda_0 \Delta} \left[\left(1 + \frac{\beta^2}{8} \right) I_0(b) - \frac{\beta}{2} (I_{-1}(b) + I_1(b)) + \frac{\beta^2}{16} (I_{-2}(b) + I_2(b)) \right] \quad (\text{A13})$$

and making use of the property

$$I_{-n}(z) = I_n(z), \quad (\text{Abramowitz \& Stegun, 1972} - 9.6.6), \quad (\text{A14})$$

we have

$$P(\Delta) = \lambda_0 e^{-\lambda_0 \Delta} \left[\left(1 + \frac{\beta^2}{8} \right) I_0(b) - \beta I_1(b) + \frac{\beta^2}{8} I_2(b) \right] \quad (\text{A15})$$

$$P(\Delta) = \lambda_0 e^{-\lambda_0 \Delta (1 - \frac{\beta}{2})} e^{-b} \left[\left(1 + \frac{\beta^2}{8} \right) I_0(b) - \beta I_1(b) + \frac{\beta^2}{8} I_2(b) \right] \quad (\text{A16})$$

Now we perform the asymptotic analysis. For large Δ we have

$$I_n(z) \sim \frac{e^z}{\sqrt{2\pi z}} \left[1 - \frac{\mu-1}{8z} + \frac{(\mu-1)(\mu-9)}{2!(8z)^2} - \frac{(\mu-1)(\mu-9)(\mu-25)}{3!(8z)^3} + \dots \right] \quad (\text{A17})$$

where $\mu = 4n^2$. And so

$$I_0(z)e^{-z} \sim \frac{1}{\sqrt{2\pi z}} \left[1 + \frac{1}{8z} + \frac{9}{128z^2} + \dots \right] \quad (\text{A18})$$

$$I_1(z)e^{-z} \sim \frac{1}{\sqrt{2\pi z}} \left[1 - \frac{3}{8z} - \frac{15}{128z^2} + \dots \right] \quad (\text{A19})$$

$$I_2(z)e^{-z} \sim \frac{1}{\sqrt{2\pi z}} \left[1 - \frac{15}{8z} + \frac{105}{128z^2} + \dots \right]. \quad (\text{A20})$$

Therefore,

$$P(\Delta) \sim \lambda_0 e^{-\lambda_0 \Delta (1 - \frac{\beta}{2})} \frac{1}{\sqrt{2\pi b}} \left[\left(1 - \frac{\beta}{2} \right)^2 + \left(1 + \frac{7\beta}{2} \right) \left(1 - \frac{\beta}{2} \right) \left(\frac{1}{8b} \right) + \frac{57\beta^2 + 60\beta + 36}{512b^2} + \dots \right] \quad (\text{A21})$$

254 The power law depends on the choice of β . In the case that $\beta = 2$ we recover $P \sim b^{-2.5}$,
255 otherwise it drops off exponentially. In Fig. A1 we plot the WTDs and corresponding
256 "local" power law estimation for various values of β .

257

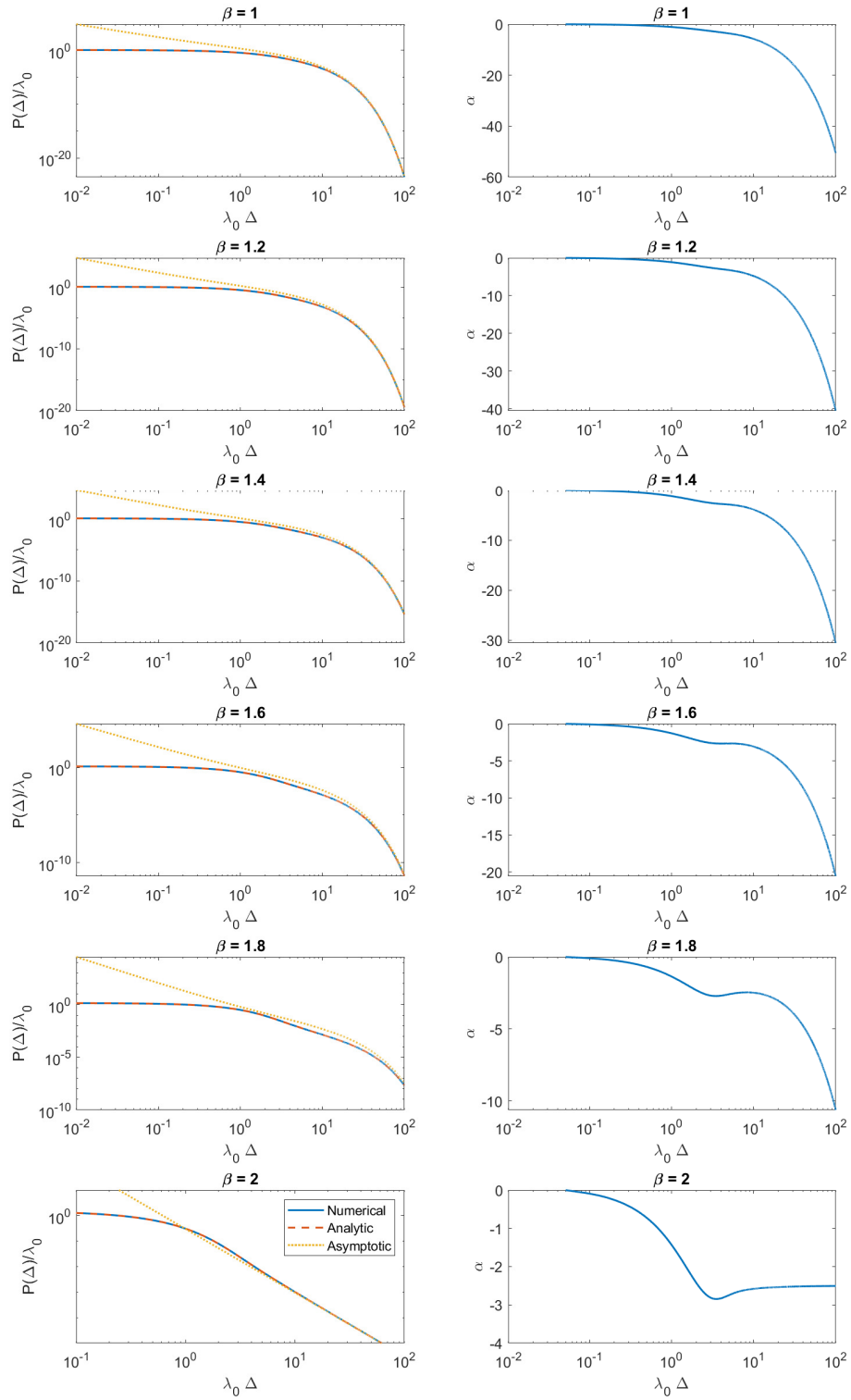


Figure A1: The left panels are the waiting time distributions with numerical and analytic solutions to eq. (A6) corresponding to various β values. The right panels are the "local" power law estimation.